Effect of nutrient media on photobiological hydrogen production by *Anabaena variabilis* ATCC 29413

Halil Berberoğlu[a], Jenny Jay[b], Laurent Pilon[a],*

[a]*Mechanical and Aerospace Engineering Department, Henry Samueli School of Engineering and Applied Science, University of California Los Angeles, Los Angeles, CA 90095, USA*
[b]*Civil and Environmental Engineering Department, Henry Samueli School of Engineering and Applied Science, University of California Los Angeles, Los Angeles, CA 90095, USA*

ARTICLE INFO

ABSTRACT

This study reports a factor 5.5 increase in hydrogen production by *Anabaena variabilis* ATCC 29413 using Allen–Arnon medium compared with BG-11 and BG-11$_0$ media. The results were obtained with a flat panel photobioreactor made of acrylic and operated in two stages at 30 °C. Stage 1 aims at converting carbon dioxide into biomass by photosynthesis while Stage 2 aims at producing hydrogen. During Stage 1, the photobioreactor was irradiated with $65\,\mu mol/m^2/s$ ($14\,W/m^2$) of light and sparged with a mixture of air (95% by volume) and carbon dioxide (5% by volume). During Stage 2, irradiance was increased to $150\,\mu mol/m^2/s$ ($32\,W/m^2$) and the photobioreactor was sparged with pure argon. The parameters continuously monitored were (1) the cyanobacteria concentration, (2) the pH, (3) the dissolved oxygen concentration, (4) the nitrate and (5) the ammonia concentrations in the medium, and (6) the hydrogen concentration in the effluent gas. The three media BG-11, BG-11$_0$, and Allen–Arnon were tested under otherwise similar conditions. The maximum cyanobacteria concentrations during Stage 2 were 1.10 and 1.17 kg dry cell/m³ with BG-11 and Allen–Arnon media, respectively, while it could not exceed 0.76 kg dry cell/m³ with medium BG-11$_0$. Moreover, the heterocyst frequency was 5%, 4%, and 9% for *A.variabilis* grown in BG-11, BG-11$_0$, and Allen–Arnon media. The average specific hydrogen production rates were about 8.0×10^{-5} and 7.2×10^{-5} kg H$_2$/kg dry cell/h (1 and 0.9 L H$_2$/kg dry cell/h at 1 atm and 30 °C) in media BG-11 and BG-11$_0$, respectively. In contrast, it was about 4.5×10^{-4} kg H$_2$/kg dry cell/h (5.6 L H$_2$/kg dry cell/h at 1 atm and 30 °C) in Allen–Arnon medium. The maximum light to hydrogen energy conversion efficiencies achieved were 0.26%, 0.16%, and 1.32% for BG-11, BG-11$_0$, and Allen–Arnon media, respectively. The larger heterocyst frequency, specific hydrogen production rates, efficiencies, and cyanobacteria concentrations achieved using Allen–Arnon medium were attributed to higher concentrations of magnesium, calcium, sodium, and potassium in the medium. Finally, presence of vanadium in Allen–Arnon medium could have induced the transcription of vanadium based nitrogenase which is capable of evolving more hydrogen than molybdenum based one.

© 2008 International Association for Hydrogen Energy. Published by Elsevier Ltd. All rights reserved.

Corresponding author. Tel.: +1 310 206 5598; fax: +1 310 206 4830.
E-mail address: pilon@seas.ucla.edu (L. Pilon).

Nomenclature

A_{abs}	mass absorption cross-section of $A.variabilis$, m^2/kg
A_s	irradiated surface area of the photobioreactor, m^2
C_{H_2}	concentration of H_2 in the effluent, kg/m^3
G_{in}	total irradiance, W/m^2
$G_{\lambda,in}$	spectral irradiance, $W/m^2/nm$
M	molecular mass, kg/mol
n	average number of oxygen atoms per carbon atom in biomass
$[NH_4^+]_{aq}$	ammonia concentration, mM
$[NO_3^-]_{aq}$	nitrate concentration, mM
p	average number of hydrogen atoms per carbon atom in biomass
P_0	total pressure, Pa
P_{H_2}	partial pressure of H_2, Pa
q	average number of nitrogen atoms per carbon atom in biomass
Q_0	the energy content of biomass per available electron, J/#e
$\dot{Q}_{out}$	volumetric flow rate of the effluent gas, mL/min
R	universal gas constant, $R = 8.314 J/mol/K$
R_{H_2}	molar rate of production of H_2, mol/s
T	temperature, K
T_λ	spectral transmittance of 6 mm acrylic sheet, %
V_L	volume of the medium, m^3
X	cyanobacteria concentration, kg dry cell/m^3

Greek symbols

γ_b	degree of reductance of the biomass
ΔG^0	standard-state free energy of formation of H_2 from water splitting reaction, J/mol
Δt	time duration between successive measurements, h
η_b	light to biomass energy conversion efficiency, %
η_{H_2}	light to H_2 energy conversion efficiency, %
μ	specific growth rate of cyanobacteria, s^{-1}
π_{H_2}	specific hydrogen production rate, L/kg/h
σ_b	mass fraction of carbon in biomass

Subscripts

avg	refers to time-averaged value
C	refers to carbon
H_2	refers to hydrogen
λ	refers to wavelength
max	refers to maximum value
PAR	refers to photosynthetically active radiation, i.e., from 400 to 700 nm

1. Introduction

The growing energy needs and concerns over air pollution and climate changes necessitate greater reliance on a combination of fossil fuel-free energy sources and on new technologies for capturing and converting carbon dioxide. Moreover, development of fuel cell technology, converting hydrogen and oxygen into electricity and water, is a promising environmentally friendly technology for portable energy sources and for transportation systems [1]. Photobiological hydrogen production by cultivation of photosynthetic microorganisms offers a clean and sustainable alternative to thermochemical or electrolytic production technologies with the added advantage of CO_2 mitigation.

The cyanobacterium *Anabaena variabilis* is a photosynthetic prokaryote listed among the potential candidates for hydrogen production [2] and, whose genome sequence has been completed [3]. *A.variabilis* utilizes light energy in the spectral range from 400 to 700 nm, known as the photosynthetically active radiation (PAR), and consumes CO_2 to produce biomass and oxygen. Under nitrogen limited conditions it produces hydrogen. *A.variabilis* and its mutants are of great research interest as hydrogen producers [2,4–8]. For example, the mutant PK84 has been genetically modified to lack the uptake hydrogenase to increase its net H_2 production rate [9]. The reader is referred to Refs. [1,2,10–13] for detailed reviews of photobiological hydrogen production.

In order to promote H_2 production by *A.variabilis*, Markov et al. [14] proposed a two stage photobioreactor alternating between (i) a growth and (ii) a H_2 production stage. During the first stage, cyanobacteria fix CO_2 and nitrogen from the atmosphere to grow and produce photosynthates. In the second stage, they utilize these photosynthates to generate H_2. The authors constructed a flat panel photobioreactor and reduced the pressure to 300 torr during the second stage to promote H_2 production. They reported a maximum specific H_2 production rate of 12.5 mL/kg dry cell/h obtained from single measurements taken every 6 days after 15 min of degassing and 5 h of illumination. However, no data on H_2 production or on microorganism concentration was reported at intermediate times between each measurement.

Similarly, Tsygankov et al. [15] constructed a helical photobioreactor made of transparent PVC tube with inner diameter of 10 mm. They operated it in two stages for photobiological H_2 production using the Allen–Arnon medium. The authors reported maximum H_2 production rates of about 2.6 and 5.1 L/kg dry cell/h for *A.variabilis* ATCC 29413 and the mutant PK84, respectively. The maximum microorganism concentrations were about 1.13 and 1.3 kg dry cell/m^3 for the wild strain and PK84, respectively.

More recently, Yoon et al. [16] also used a two stage photobioreactor and suggested an improvement on the first stage by incorporating nitrate in the growth medium (medium BG-11) for faster growth of *A.variabilis*. The authors constructed two flat panel photobioreactors of thickness 2 and 4 cm made of polyacrylate having a total volume of 450 mL and 900 mL, respectively. Moreover, they used argon sparging during the second stage to promote H_2 production as opposed to vacuum used by Markov et al. [14]. The authors reported maximum specific H_2 production rates of 4.1 and

0.45 L/kg dry cell/h for the 2 cm and the 4 cm thick photobioreactor, respectively. The corresponding maximum cyanobacteria concentrations reported were 0.8 and 1.2 kg dry cell/m^3. The authors operated the photobioreactor for 40 h in the second stage and reported a total volume of 40 mL of hydrogen.

Due to differences in (i) the designs of the photobioreactors, (ii) the light sources, (iii) the temperature of operation, (iv) the strains, and (v) the media used, the results reported in the literature for H_2 production show large variation. Moreover, these differences make it difficult to compare and understand the effect of each parameter on the observed biomass and H_2 production rates and efficiencies. Among these parameters the effect of the growth media has not been addressed. Therefore, the objective of this paper is to compare the growth and H_2 production performances of *A.variabilis* ATCC 29413 cultivated in three different media namely BG-11, BG-11$_0$, and Allen–Arnon while all other parameters are kept the same.

2.   Materials and methods

2.1.   Growth media

The three media investigated in the present study were (i) BG-11, or ATCC medium 616, (ii) BG-11$_0$, and (iii) Allen–Arnon medium. To facilitate the comparison, Table 1 summarizes the composition of each medium. Only medium BG-11 contained nitrate whereas the other media were used to grow *A.variabilis* under nitrogen fixing conditions. All media were prepared according to the recipes provided by Meeks [17]. Finally, the ionic strengths of BG-11, BG-11$_0$, and Allen–Arnon media were estimated to be 5.31, 2.31, and 14.00 mM, respectively.

2.2.   Photobioreactor and instrumentation

A flat panel photobioreactor made of acrylic was constructed and instrumented to monitor and compare the growth and hydrogen production by *A.variabilis* using the three different nutrient media under otherwise similar conditions. The measured operating parameters of the single biosolar panel were (1) the CO_2 and H_2 concentrations in the gas phase, (2) the irradiance, (3) the head-space pressure, (4) the reactor temperature, (5) the cyanobacteria concentration, (6) the pH, the (7) dissolved O_2, (8) nitrate, and (9) ammonia concentrations in the medium.

A schematic of the experimental setup is shown in Fig. 1. The photobioreactor was made from 6 mm thick acrylic sheets, separated by a distance of 4.5 cm in the direction of light propagation, and designed to have a total volume of 1.35 L. Ports were placed on top of the panel for (i) measuring the head-space pressure and (ii) the reactor temperature, (iii) sampling the head-space, and (iv) removing the generated gases. The head-space pressure was measured with a gauge type electronic pressure sensor (PX26 by Omega Engineering, USA) connected to a data acquisition board (Personal DAQ/55 by Iotech, USA). The pressure sensor was calibrated with a pressure calibrator (PCL 4000 by Omega Engineering, USA)

Nutrient	Concentration in medium (mg/L)		
	BG-11	BG-11$_0$	Allen and Arnon
K_2HPO_4	29.6	29.6	268
$MgSO_4 \cdot 7H_2O$	72.7	72.7	250
$CaCl_2 \cdot 2H_2O$	34.9	34.9	75.0
NaCl	0	0	250
KOH	0	0	7.56
Ferric ammonium citrate	5.82	5.82	0
Citric acid $\cdot 1H_2O$	5.82	5.82	0
$NaNO_3$	255	0	0
$FeSO_4 \cdot 7H_2O$	0	0	19.9
$Na_2 EDTA \cdot 2H_2O$	0.970	0.970	29.7
$MnCl_2 \cdot 4H_2O$	1.76	1.76	1.80
MoO_3	0.017	0.017	0.180
$ZnSO_4 \cdot 7H_2O$	0.215	0.215	0.220
$CuSO_4 \cdot 5H_2O$	0.077	0.077	0.079
H_3BO_3	2.77	2.77	2.86
NH_4VO_3	0	0	0.023
$CoCl_2 \cdot 6H_2O$	0.048	0.048	0.040

Table 1 – Concentrations of nutrients in the three different media investigated

and measured the pressure with an accuracy of ± 0.1 Pa. The reactor temperature was measured with a K-type thermocouple in a stainless steel jacket (KMTSS-040U-6 by Omega Engineering, USA). The calibration of the thermocouple was validated at the boiling temperature of water (100 °C) and at the melting temperature of ice (0 °C) at atmospheric pressure. The temperature of the photobioreactor was maintained at 30 ± 1 °C with a closed loop temperature control achieved with the feedback from the thermocouple and four 300 W cartridge heaters (CIR-1032 by Chromalox, USA) located at the bottom of the photobioreactor. Moreover, the exhaust pipe was made of a stainless-steel pipe of diameter 4.76 mm and wall thickness of 0.71 mm and had a sampling port for analyzing the composition of the effluent gas. The exhaust pipe was immersed in a flask containing water to prevent the flow of ambient air into the photobioreactor.

In addition, the photobioreactor featured an illumination area of 300 cm^2. The illumination was provided by fluorescent light bulbs (Fluorex by Lights of America, USA). The irradiance was measured at the outside surface of the photobioreactor with a quantum sensor (LI-190SL by LI-COR Inc., USA) that measures the total irradiance with an accuracy of $\pm 1 \mu mol/m^2/s$ (± 0.21 W/m^2) in the PAR spectral range, i.e., from 400 to 700 nm. Moreover, the spectral irradiance of the fluorescent light bulbs were measured with a spectrophotometer (model USB2000, Ocean Optics) connected to a cosine collector over the spectral range from 350 to 750 nm. Fig. 2 shows (i) the transmittance T_λ of a 6 mm acrylic sheet, (ii) the irradiance provided by the fluorescent light bulbs $G_{\lambda,in}$ normalized by its maximum value $G_{max,in}$ at $\lambda_{max} = 542$ nm, and (iii) the absorption cross-section of *A.variabilis* $A_{abs,\lambda}$ normalized by its maximum value $A_{abs,max}$ over the spectral range from 300 to 800 nm [18]. Fig. 2 indicates that the acrylic
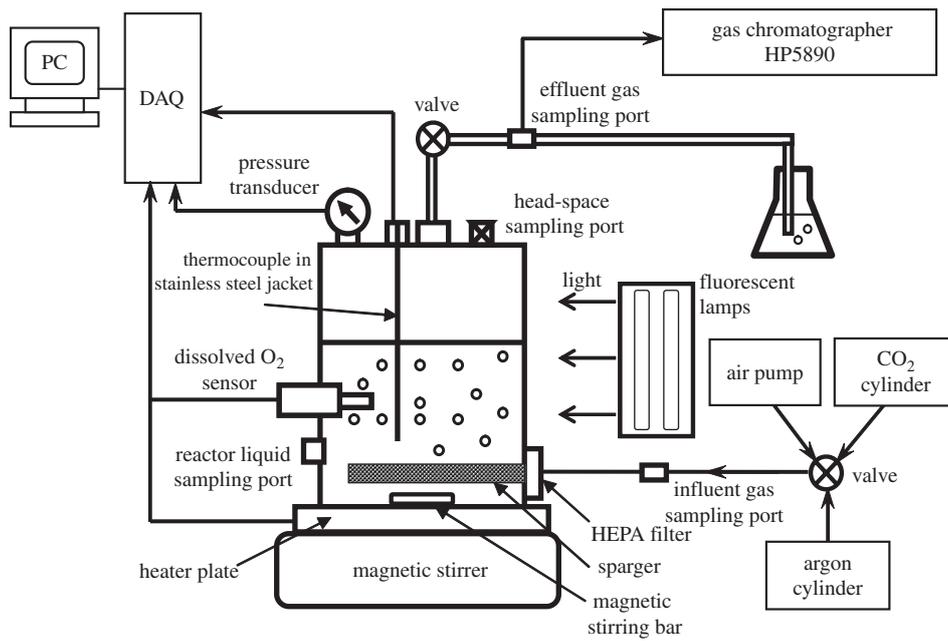
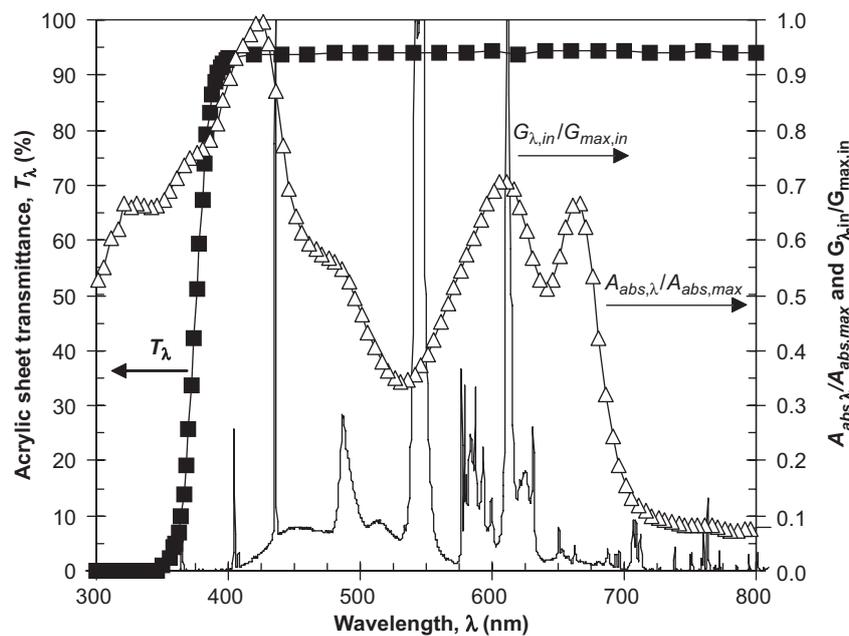Fig. 1 – Schematic of the front view of the experimental setup and instrumentation.

Fig. 2 – The spectra of (i) the transmittance T_λ of a 6 mm acrylic sheet (■), (ii) the absorption cross-section of *A.variabilis* normalized by its maximum value $A_{\mathrm{abs},\lambda}/A_{\mathrm{abs,max}}$ (△), and (iii) the irradiance provided by the fluorescent light bulbs normalized by its maximum value $G_\lambda/G_{\mathrm{max}}$ (solid line) over the spectral range from 300 to 800 nm.

sheet transmits 95% of the incident light from 390 to 800 nm. This appears to be adequate for cultivating *A.variabilis* which features absorption peaks within the spectral region from 400 to 700 nm [18]. Moreover, the fluorescent lamps provided adequate emission in the PAR with negligible emission in the IR, making them a suitable light source for the experiments. The irradiance was controlled by changing the number of metal screens in front of the light bulbs. These screens partially block the light, lowering the total irradiance incident on the photobioreactor without changing the spectrum of the transmitted light in the spectral range from 300 to 800 nm as verified experimentally.

Furthermore, the concentrations of CO_2 and H_2 in the effluent gas were measured with a gas chromatographer (HP-5890 by Hewlett Packard, USA) equipped with a packed column (Carboxen-1000 by Supelco, USA) and a thermal

conductivity detector (TCD). The gas chromatographer output was processed with an integrator (HP-3395 by Hewlett Packard, USA). Throughout the gas analysis, the injector and detector temperatures were maintained at 120 °C. During the H_2 analysis, argon was used as the carrier gas and the oven temperature was maintained at 35 °C. On the other hand, during the CO_2 analysis, helium was used as the carrier gas and the oven temperature was maintained at 255 °C. The retention times for H_2 and CO_2 were 2.1 and 4.9 min, respectively. Calibration curves for the TCD response were prepared at seven different known gas concentrations at atmospheric pressure from 16×10^{-6} to $3.2 \times 10^{-3}\,kg/m^3$ for H_2, and from 3.96×10^{-3} to $352 \times 10^{-3}\,kg/m^3$ for CO_2. All calibration curves were linear within these ranges of gas concentrations. During the experiments, peak heights were recorded and correlated with the corresponding gas concentrations using the respective calibration curves. The accuracy of the gas chromatographer was estimated to be $\pm 2 \times 10^{-6}\,kg/m^3$.

In addition, a septum valve located on the side of the reactor enabled the sampling of the reactor liquid with a syringe. Then, at regular time intervals (i) the cyanobacteria concentration, (ii) the pH of the reactor medium, (iii) the nitrate, and (iv) the ammonia concentrations were measured. The cyanobacteria concentration were determined by measuring the optical density (OD) of the medium. These measurements were performed at 683 nm in disposable polystyrene cuvettes with light path of 10 mm using a UV-visible spectrophotometer (Cary-3E by Varian, USA) along with calibration curves prepared for *A.variabilis* grown in each media. Fig. 3 shows the calibration curves relating the dry cell weight X to the OD at 683 nm for *A.variabilis* and indicates that one unit of OD corresponds to $0.244\,kg\,dry\,cell/m^3$ in all media. The calibration curve is valid for concentrations up to about $0.3\,kg\,dry\,cell/m^3$ corresponding to an OD of about 1.4. In order to quantify higher cell concentrations, the sample

from the photobioreactor was diluted by a known factor until the measured OD was less than 1.4. The pH was measured using a pH electrode with a sensitivity of ± 0.01 pH (Calomel 7110BN by Thermoelectron Company, USA). The nitrate and the ammonia concentrations were measured with nitrate and ammonia ion sensitive probes Electrode-ise Nitrate and Electrode-ise Ammonia both by Denver Instrument Company, USA. The response of each probe was calibrated by stock solutions of concentrations 0, 0.167, 1.67, and 15 mM thus, covering the range of concentrations expected during the photobioreactor operation. Both probes had a precision of $1\,\mu M$. Finally, the dissolved O_2 concentration in the medium $[O_2]_{aq}$ was measured with a dissolved O_2 probe (Fisher Brand Dissolved Oxygen meter, Fisher Scientific, USA) mounted on the side of the photobioreactor. It had an accuracy of $4\,\mu M$.

Finally, the mixing of the cyanobacterial suspension in the photobioreactor was achieved by a 3.5 cm long magnetic stirring bar, a magnetic stirrer (Isotemp by Fisher Scientific, USA), and a gas sparger (Bubble Wall by PennPlax, USA). The sparger received gas from a gas mixer providing the desired relative concentrations of air and CO_2, or argon sterilized through a HEPA filter of pore size $0.3\,\mu m$ (HEPA-Vent by Whatman, USA). The gas mixer assembly comprised three flow meters (FL-120 by Omega Heater Company, USA), three metering valves (MS-01-79 by Swagelock, USA) for controlling the flow rates of each gas, and three unidirectional valves (Check-valve by Aqua Culture, USA) preventing back flow of gases. In addition, the composition of the influent gas mixture was collected through the gas sampling port located before the HEPA filter and analyzed using the gas chromatographer.

Prior to operation, the photobioreactor was tested for H_2 leakage. To do so, it was filled with 700 mL of distilled water and the head-space was filled with a mixture of H_2 (2% by volume) and air (98% by volume) at 1 atm. After the head-space pressure was stabilized, indicating equilibrium between the gas and the liquid phases, the head-space was sampled and the H_2 concentration was measured as a function of time. Fig. 4 shows the concentration of H_2 retained in the head-space relative to its initial value over the course of four days. It indicates that about 95% of the H_2 was retained in the head-space after about two days. Moreover, during the H_2 production stage, the photobioreactor was continuously sparged with pure argon and the produced H_2 was carried out at a much faster rate than it could diffuse out of the acrylic walls. Thus, loss of H_2 by diffusion out of the acrylic walls was assumed to be negligible. Finally, owing to the fact that CO_2 and O_2 are larger molecules than H_2, the diffusion coefficients of these species through the acrylic walls are smaller than that of H_2 [19]. Therefore, losses of all these species from the photobioreactor were assumed to be much smaller than losses of H_2 and could safely be ignored.

2.3. Operation of the flat panel photobioreactor

The photobioreactor was operated in two stages, where during Stage 1 microorganisms consumed CO_2 and produce biomass, and during Stage 2 they produced H_2. First, the photobioreactor was sterilized by flushing with sodium hypochlorite for 30 min and rinsing for 30 min with HEPA
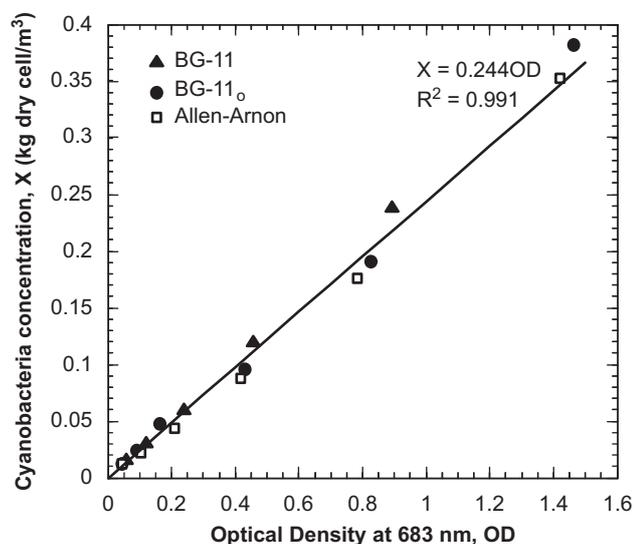

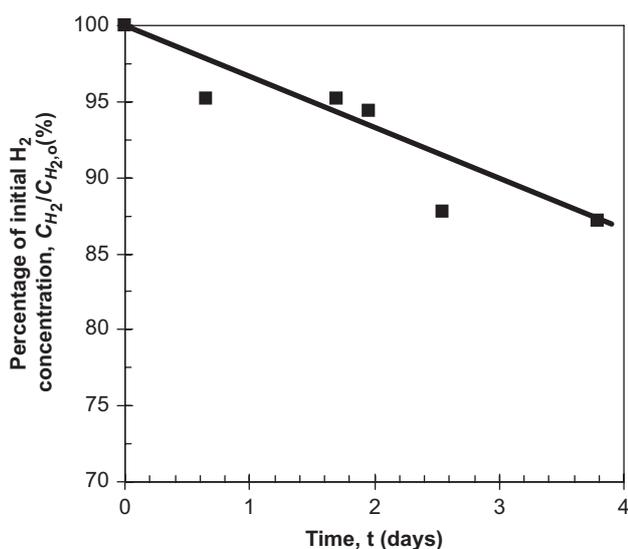Fig. 3 – Calibration curve for the dry cell weight versus the OD of *A.variabilis* at 683 nm in all media.

Fig. 4 – Percentage of the initial H_2 concentration retained in the photobioreactor over the course of four days. The solid line corresponds to a linear fit to the data.

filter sterilized deionized water. Then, 700 mL of media was supplied to the photobioreactor. The sparger was turned on at a flow rate of 170 ± 1 mL/min and the sparging gas composition was adjusted to 95 vol.% air and 5 vol.% CO_2. The total PAR irradiance on the outside surface of the photobioreactor was set to 65 ± 2 µmol/m^2/s (i.e., 4700 lux or 14 W/m^2) and the temperature controller was set to 30 °C. Once the photobioreactor temperature reached steady state, 50 mL of actively growing culture of *A.variabilis* was injected in the photobioreactor. The inoculum for each experiment was grown in their respective media under 28 µmol/m^2/s (2000 lux or 5.9 W/m^2) irradiation. The first stage continues until (i) the nitrate concentration vanished in the case of BG-11, (ii) the microorganisms stopped growing in the case of BG-11$_0$, and (iii) the microorganism concentration reached 1.1 kg dry cell/m^3 in the case of Allen–Arnon medium. Then, the photobioreactor was sparged with pure argon (99.99% purity) at a flow rate of 45 ± 1 mL/min, and the total irradiance was increased to 150 ± 5 µmol/m^2/s (i.e., 11,000 lux or 32 W/m^2) by reducing the number of metal wire screens placed in front of the lamps. This second stage ended when H_2 production by *A.variabilis* ceased.

2.4. Performance assessment

In order to assess the performance of the photobioreactor, the specific hydrogen production rate as well as the conversion efficiencies of light to hydrogen energy and light to biomass energy were computed.

2.4.1. Light to biomass energy conversion efficiency
The instantaneous light to biomass energy conversion efficiency is defined as [20],

$$\eta_b = \frac{(V_L \sigma_b \gamma_b Q_0)/M_C}{G_{PAR,in} A_s} \frac{dX}{dt}, \tag{1}$$

where dX/dt is the time rate of change of the microorganism concentration, expressed in kg dry cell/m^3/s. This rate is estimated by the second-order centered-difference method at the mid-point between two consecutive data points [21]. The volume of the cyanobacterial suspension in the photobioreactor is denoted by V_L and initially equals to 0.7×10^{-3} m^3. Furthermore, Q_0 is the energy content of biomass per available electron, equal to 112,800 J/#e for *A.variabilis* PK84 [22] and M_C is the molar mass of carbon equal to 0.012 kg/mol. Moreover, σ_b is the mass fraction of carbon in the biomass and γ_b is the degree of reductance of the biomass, i.e., the number of available electrons per mol of carbon in the biomass, expressed in #e/mol. The values of σ_b and γ_b depend on the elemental composition of the biomass given as $CH_pO_nN_q$, where p, n, and q are the average numbers of hydrogen, oxygen, and nitrogen atoms per carbon atom in the biomass. The elemental composition of *A.variabilis* PK84 was reported by Tsygankov et al. [22], as $CH_{2.11}O_{0.485}N_{0.159}$ corresponding to σ_b equals to 0.498. It is assumed that the same values hold for the wild strain used in the present study by analogy with Tsygankov et al. [22]. In addition, the degree of reductance is defined as $\gamma_b = 4 + p - 2n - 3q$ and is equal to 4.663 #e/mol for *A.variabilis* [23]. Finally, $G_{PAR,in}$ is the total PAR irradiance incident on the photobioreactor of surface area A_s.

2.4.2. Specific hydrogen production rate
The specific hydrogen production rate π_{H_2} is defined as,

$$\pi_{H_2} = \frac{C_{H_2} \dot{Q}_{out}}{X V_L}, \tag{2}$$

where C_{H_2} is the concentration of H_2 measured in the effluent expressed in kg/m^3 and $\dot{Q}_{out}$ is the volumetric flow rate of the effluent gas. From mass conservation, $\dot{Q}_{out}$ is equal to the flow rate of Argon set at 45 ± 1 mL/min. In order to make the comparison easier with the results reported in the literature [14–16,22], the unit of π_{H_2} is converted from kg H_2/kg dry cell/s to L/kg dry cell/h assuming that 1 kg of H_2 occupies 12.43×10^3 L at 1 atm and 30 °C.

2.4.3. Light to hydrogen energy conversion efficiency
The light to hydrogen energy conversion efficiency is expressed as [24]

$$\eta_{H_2} = \frac{[\Delta G^0 - RT \ln(P_0/P_{H_2})]C_{H_2} \dot{Q}_{eff}/M_{H_2}}{G_{PAR,in} A_s}, \tag{3}$$

where ΔG^0 is the standard-state free energy of formation of H_2 from the water splitting reaction. It is equal to 236,337 J/mol at 303 K. The term $RT \ln(P_0/P_{H_2})$ is the correction factor for ΔG^0 when H_2 production takes place at H_2 partial pressure P_{H_2} instead of the standard pressure P_0 of 1 atm. Finally, M_{H_2} is the molecular weight of H_2 equals to 2×10^{-3} kg/mol.

3. Results

The results obtained during the two stage operation of the flat panel photobioreactor using the three different media are summarized in Table 2 and are discussed in the following sections.

Table 2 – Summary of the major results obtained for *A.variabilis* ATCC 29413 during two stage operation of the 4.5 cm thick and 700 mL flat panel photobioreactor using the three different media

	BG-11	BG-11$_0$	Allen and Arnon
X_{max} (kg/m^3)	1.10	0.76	1.17
$\eta_{b,max}$ (%)	10.48	9.68	9.82
$\eta_{b,avg}$ (%)	7.48	5.60	6.91
$\pi_{H_2,max}$ (L/kg/h)	1.40	1.42	7.73
$\pi_{H_2,avg}$ (L/kg/h)	1.03	0.89	5.59
$\eta_{H_2,max}$ (%)	0.26	0.16	1.32
$\eta_{H_2,avg}$ (%)	0.19	0.11	0.96
$V_{H_2,tot}$[a] (mL)	150	80	750

[a] Over approximately 8 days.

3.1. Cyanobacteria and nitrate concentrations

Fig. 5(a) shows the concentration of *A.variabilis* in the photobioreactor as a function of time for all media during the two-stage operation. It indicates that in medium BG-11 the cyanobacteria concentration increased almost linearly with time, indicating that light was a limiting factor during growth [15,16]. The nitrate concentration (not shown) decreased from 2.9 to 0 mM during the growth phase in BG-11 while it was zero at all times for the other two media. For BG-11, once the nitrate concentration vanished, the cyanobacteria concentration reached a relatively constant value of 1.1 kg dry cell/m^3 after about 110 h when Stage 1 was experimentally ended. However, in the case of medium BG-11$_0$, the microorganism concentration could not exceed 0.75 kg dry cell/m^3. Then, the photobioreactor was changed to the second stage after approximately 115 h. Furthermore, as indicated by the slopes of the growth curves in Fig. 5(a), in absence of nitrate (media BG-11$_0$ and Allen–Arnon), the average growth rate of the microorganisms was smaller than when nitrate was present. However, despite the absence of nitrate in the Allen–Arnon medium, the yield was not inhibited unlike in BG-11$_0$. In order to keep the irradiance within the photobioreactor similar to that prevailing in medium BG-11, the second stage started when the cyanobacteria concentration reached the same value of 1.1 kg dry cell/m^3. Moreover, the microorganisms reached this concentration approximately at the same time as in BG-11.

3.2. Light to biomass energy conversion efficiency

Fig. 5(b) illustrates the light to biomass energy conversion efficiency, η_b, of the photobioreactor as a function of time during the two stage operation for all three media. It indicates that for medium BG-11, η_b was initially 10.5% and continually decreased to zero during the growth stage. The associated time-averaged light to biomass energy conversion efficiency during Stage 1 was 7.48%. On the other hand, with medium BG-11$_0$ the maximum η_b achieved was only 9.68% and the time-averaged value was 5.60%. Finally, for Allen–Arnon

medium, η_b initially was 5.75% and increased continually to approximately 9.8% after about 100 h beyond which the growth slowed and η_b decreased to approximately 4.5%. The time-averaged η_b during Stage 1 was 6.91%. Once the photobioreactor was changed to the Stage 2, η_b decreased to values smaller than 0.5% but did not completely vanish.

3.3. Specific H$_2$ production rates

Fig. 5(c) shows the specific H$_2$ production rate, π_{H_2}, of *A.variabilis* as a function of time for all media. Each point in the figure corresponds to the average of six measurements taken during the course of 24 h. It indicates that the specific H$_2$ production rate in Allen–Arnon medium was 5.5 times larger than that in the BG-11 medium for similar cyanobacteria concentrations. However, the difference between π_{H_2} observed in BG-11 and BG-11$_0$ were not significantly different. The time-averaged specific H$_2$ production rates over the entire duration of the second stage were 1.03, 0.89, and 5.59 L/kg dry cell/h for the media BG-11, BG-11$_0$, and Allen–Arnon, respectively. Moreover, the total volume of H$_2$ produced during each experiment, estimated by integrating R_{H_2} over time, was 150, 80, and 750 mL, respectively, for a total liquid volume of 700 mL. Finally, when changed to the second stage, photobioreactor containing Allen–Arnon medium started producing H$_2$ within the next hour whereas a time delay of about 12 h was observed for media BG-11 and BG-11$_0$.

3.4. Light to H$_2$ energy conversion efficiency

Trends similar to specific hydrogen production rates were observed for the light to H$_2$ energy conversion efficiencies η_{H_2} as illustrated in Fig. 5(d). The maximum light to H$_2$ energy conversion efficiency, $\eta_{H_2,max}$, observed during the experiments was 1.32% with the Allen–Arnon medium. On the other hand, it was 0.26% and 0.16% for media BG-11 and BG-11$_0$, respectively. The time-averaged η_{H_2} over the entire second stage of approximately 8 days was 0.19%, 0.11%, and 0.96% for the BG-11, BG-11$_0$, and Allen–Arnon media, respectively.

3.5. Dissolved O$_2$, pH, and ammonia concentrations

Fig. 5(e) shows the concentration of the dissolved O$_2$ in the photobioreactor as a function of time for the three media investigated during the two stage operation. It indicates that during the first stage, the dissolved O$_2$ concentration $[O_2]_{aq}$ started increasing from about 240 ± 4 to 260 ± 4 μM as the cyanobacteria concentration increased in the photobioreactor. This can be attributed to the O$_2$ production by *A.variabilis* during photosynthesis. Moreover, when sparged with argon, the dissolved O$_2$ concentration decreased to values below 3 μM and subsequently vanished for the rest of the second stage. Similarly, Fig. 5(f) shows the medium pH as a function of time. During the first stage the pH was about 6.9 ± 0.1 while it increased to 7.5 ± 0.1 during the second stage for all media. Finally, the measurements taken with the ammonia sensitive probe (data not shown) indicated that ammonia concentration $[NH_4^+]_{aq}$ was effectively zero for all media throughout the operation of the photobioreactor.
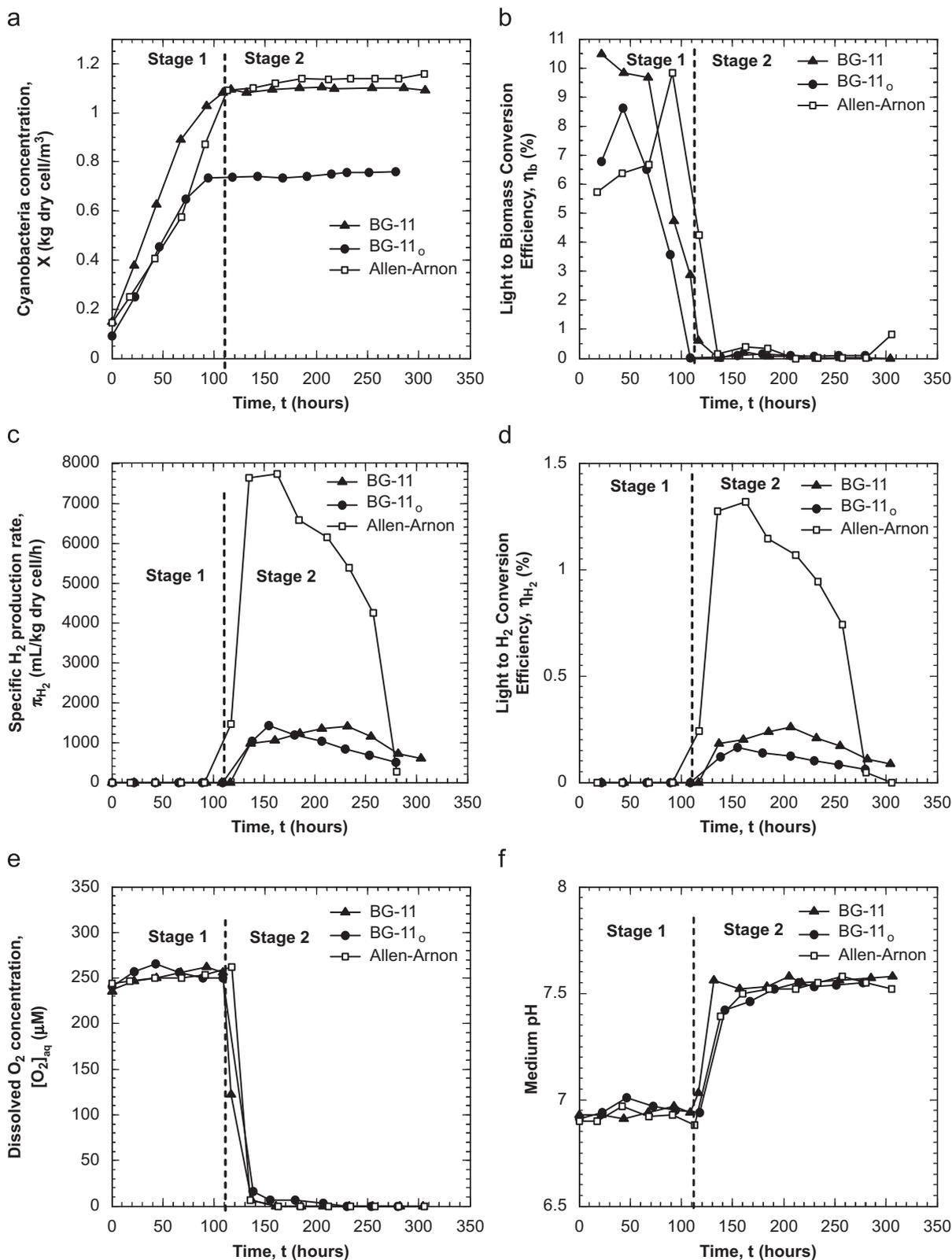
Fig. 5 – (a) Cyanobacteria concentration, (b) light to biomass energy conversion efficiency, (c) specific H_2 production rate, (d) light to H_2 energy conversion efficiency, (e) dissolved O_2 concentration, and (f) the medium pH as functions of time during two-stage photobioreactor operation for all media investigated.

3.6. Two cycle operation

Finally, in the case of Allen–Arnon medium, a second cycle of Stages 1 and 2 was performed following the end of the first cycle, i.e., when the H_2 production ceased. The first cycle lasted approximately 13 days and the second cycle 14 days. Fig. 6 presents the performance of the photobioreactor using the Allen–Arnon medium, over two cycles of alternating growth and H_2 production stages. During the first cycle, the first and second stages were run from 0 to 110 h and from 110 to 305 h, respectively. During the second cycle, the first and second stages were run from 305 to 470 h and from 470 to 640 h, respectively. Figs. 6(a) and (b) indicate that (i) most of the growth took place during Stage 1 of the first cycle and (ii) growth was very small during the second cycle, when η_b was less than 1%. On the other hand, during Stage 2 of the second cycle, 75% of the H_2 production rate of the first cycle was recovered. Then, the maximum and average specific H_2 production rates were approximately 4.75 and 3.50 L/kg dry-cell/h, respectively. Similarly, the maximum and time-averaged light to H_2 energy conversion efficiencies were 0.92% and 0.73%, respectively, during the second cycle. Finally, Figs. 6(e) and (f) show that both the dissolved O_2 concentration and the pH of the medium during the two cycles were similar to one another.

4. Discussion

4.1. Cyanobacteria and nitrate concentrations

The results shown in Fig. 5(a) indicate that addition of $NaNO_3$ was necessary to achieve high cyanobacteria yields using the medium $BG-11_0$ while this was not the case for Allen–Arnon medium. This is partly attributed to the fact that *macronutrients* such as sodium, potassium, magnesium, or calcium can be limiting components in the process of nitrogen fixation. For example, Allison et al. [25] reported that calcium is a necessary nutrient when the cyanobacteria *Nostoc muscorum* is growing under nitrogen fixing conditions and that growth does not take place in its absence. Table 1 shows that the concentrations of calcium, magnesium, and potassium in Allen–Arnon medium was, respectively, about 2, 3, and 9 times larger than in BG-11 and $BG-11_0$. In addition to the *macronutrients*, the concentration of the *micronutrient* molybdenum, which is important in the synthesis of Mo-nitrogenase [1], was about 10 times smaller in media BG-11 and $BG-11_0$ than in Allen–Arnon medium. Furthermore, the micronutrient vanadium, which is a component of the vanadium based nitrogenase enzyme [1], was missing altogether in media BG-11 and $BG-11_0$.

4.2. Light to biomass energy conversion efficiency

Bolton and Hall [26] reported the theoretical maximum efficiency of photosynthesis in converting solar radiation over the entire emission spectrum of the sun into biomass to be between 8% and 9%. This is equivalent to an efficiency between 18.5% and 20% when radiation only in the spectral range from 400 to 700 nm (PAR) is considered [26]. In the present study the light to biomass energy conversion efficiencies were calculated for the PAR. Thus, the maximum value of 10.48% with BG-11 appears to be about half of the theoretical maximum of 20% reported by Bolton and Hall [26].

As indicated in Eq. (1), the light to biomass conversion efficiency is directly related to the growth rate of the microorganisms. In addition, higher growth rates can be achieved in media containing nitrate as reported by Yoon et al. [4]. This explains the larger light to biomass conversion efficiency observed with BG-11 compared with both $BG-11_0$ and Allen–Arnon media. The difference between the biomass conversion efficiencies of $BG-11_0$ and Allen–Arnon is less significant until the cyanobacterial growth stops in $BG-11_0$ while it continues in Allen–Arnon. Uncertainty may also be introduced by the difficulty in accurately estimating the time derivative dX/dt in Eq. (1) from a discrete set of data points.

4.3. Specific H_2 production rates

Despite the difference in the cyanobacterial growth, the media BG-11 and $BG-11_0$ showed similar specific H_2 production rates [Fig. 5(c)]. On the other hand, the specific H_2 production rate achieved with the Allen–Arnon medium was 5.5 times larger. First, the effect of light transfer within the photobioreactor can be ignored because (i) all media have similar absorbances and (ii) the same microorganism concentrations were achieved in BG-11 and Allen–Arnon media resulting in similar local irradiance [27]. Moreover, Figs. 5(e) and (f) indicate that both the dissolved O_2 concentrations and pH of the media were similar from one medium to another. Finally, the temperature was kept constant at 30 °C for all media. Therefore, the observed difference in the specific H_2 production rates is attributed to the differences in the media composition. Indeed, hydrogen production by *A.variabilis* is mainly due to the nitrogenase enzymes [1]. In particular, Kentemich et al. [28] reported that *A.variabilis* can express vanadium based nitrogenase depending on the molybdenum and vanadium content of the nutrient medium. The authors stated that cultures with vanadium based nitrogenase evolved more H_2 than the molybdenum based ones. Moreover, in an independent study Tsygankov et al. [15] reported that vanadium based nitrogenase enzyme was more robust for H_2 production. Thus, one reason for the higher specific H_2 production rates observed in Allen–Arnon medium could be attributed to the presence of vanadium.

In addition, during the course of the experiments pictures of the microorganisms were taken under an optical microscope. Using the methodology suggested in Ref. [29], more than 1000 cells were counted from each media and the heterocyst frequency was estimated at 5%, 4%, and 9% in BG-11, $BG-11_0$, and Allen–Arnon medium, respectively. It represents the ratio of the number of heterocysts to the total number of cells. Fig. 7 shows the representative pictures taken from each media. It demonstrates that the heterocyst frequency was larger in Allen–Arnon medium than those observed in the other two media. It is known that the nitrogenase enzyme which is responsible for hydrogen production is located in the heterocysts [12]. Thus, this observation indicates that Allen–Arnon medium promotes also higher frequency of heterocyst differentiation under the
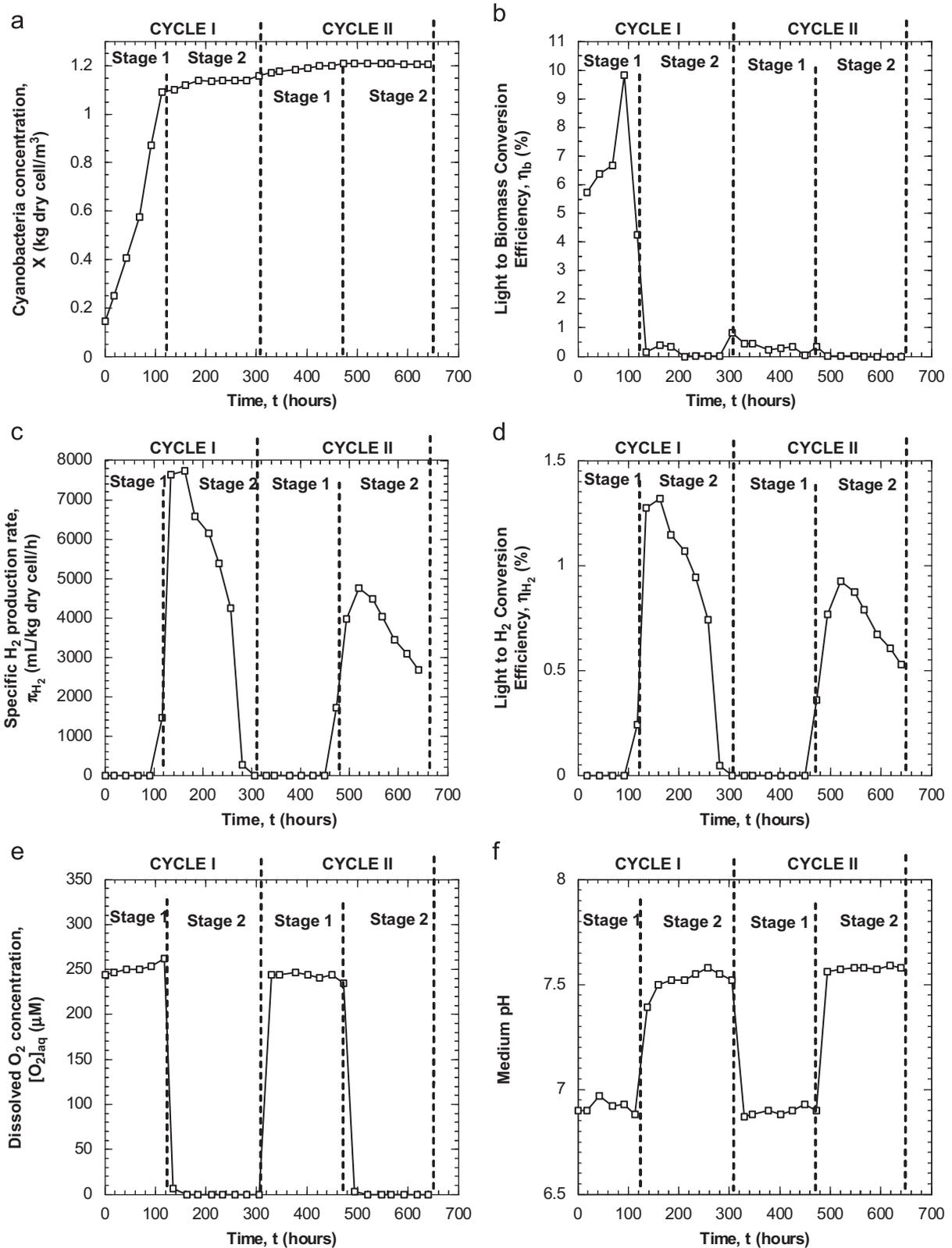
Fig. 6 – (a) Cyanobacteria concentration, (b) light to biomass energy conversion efficiency, (c) specific H_2 production rate, (d) light to H_2 energy conversion efficiency, (e) dissolved O_2 concentration, and (f) the medium pH as functions of time using the Allen–Arnon medium over two cycles.
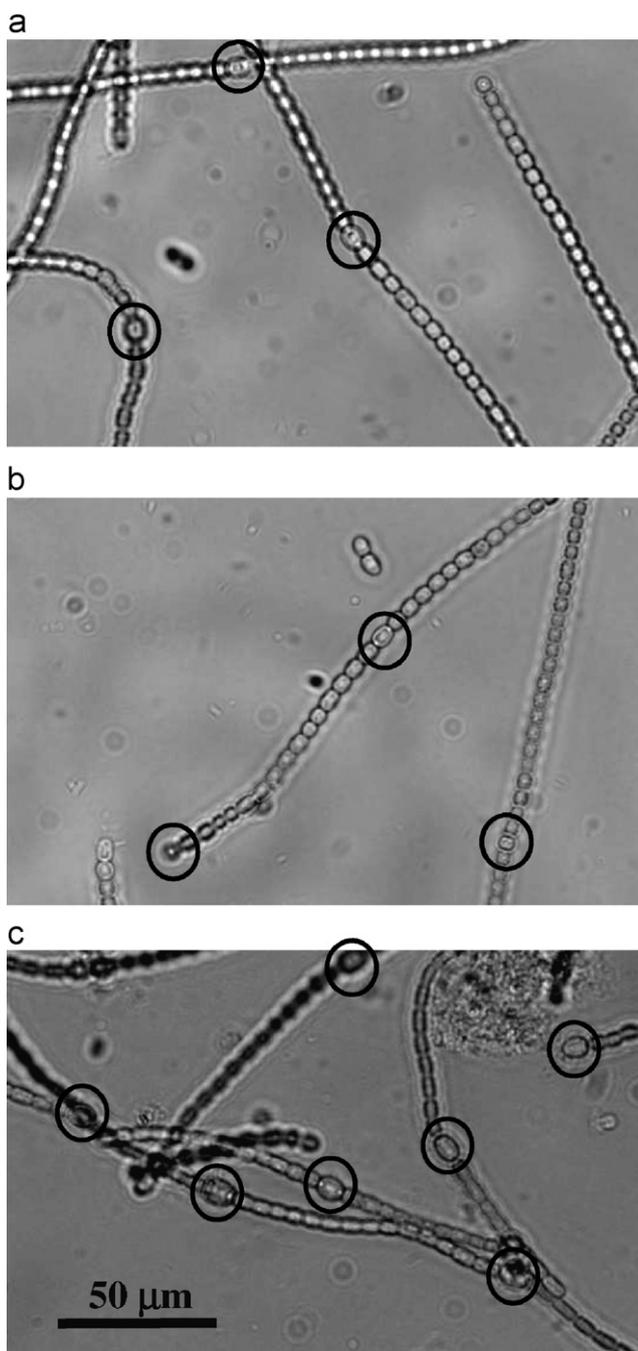
Fig. 7 – Micrographs of A.variabilis grown in (a) BG-11, (b) BG-11_0, and (c) Allen–Arnon media. The circled cells indicate the heterocysts.

identical operating conditions used, enabling higher specific hydrogen production rates.

Finally, despite the fact that the ionic strength of BG-11 was almost twice that of BG-11_0, the observed specific H_2 production rates were similar in both media. This suggests that ionic strength was not an important parameter in H_2 production. However, it can be an important factor in the overall growth of the microorganisms. Note that a parametric study of each nutrient would be needed to find the optimum media composition that maximizes the H_2 production rates,

efficiencies, and cyanobacteria concentrations. However, this falls beyond the scope of the present study.

4.4. Light to H_2 energy conversion efficiency

Despite the improved light to H_2 energy conversion efficiency achieved with the Allen–Arnon medium, the maximum value observed was about 12 times smaller than the maximum theoretical value of 16.3% reported by Prince and Kheshgi [1] for indirect biophotolysis using nitrogenase. The authors reported this value for H_2 production using 680 nm mono-chromatic light and the nitrogenase enzyme during indirect biophotolysis. Usually, the low efficiencies are attributed to limited light penetration [11,16,30]. However, Fig. 5(d) indicates that the medium composition can also drastically affect the H_2 production efficiency.

4.5. Two cycle operation

The light to biomass conversion efficiency was less than 1% during the second cycle. This is likely due to the depletion of nutrients and to the limited light penetration within the photobioreactor containing high microorganism concentration of about 1.1 kg dry cell/m^3 in the second cycle. In addition, the specific H_2 production rates and efficiencies during the second cycle were approximately 25% lower than those during the first cycle. This may be due to the low light to biomass conversion efficiency during the second cycle resulting in small photosynthate production unable to fully sustain the subsequent H_2 production stage [7]. Addition of the depleted nutrients between cycles and improving the light delivery within the photobioreactor might increase the H_2 production rate during the repeated H_2 production stages.

5. Conclusions

This paper reports for the first time the effect of the nutrient media BG-11, BG-11_0, and Allen–Arnon on H_2 production by *Anabaena variabilis* grown in a flat panel photobioreactor under otherwise similar conditions. It reports an increase (i) in the heterocyst frequency by close to a factor 2 and (ii) in the specific H_2 production rate of *A.variabilis* by a factor of 5.5 when grown in Allen–Arnon medium compared with BG-11 and BG-11_0. The following conclusions can be drawn:

1. High cyanobacteria concentrations could be reached with Allen–Arnon medium under nitrogen fixing conditions. By contrast, the presence of nitrate was essential for achieving high microorganism concentrations with medium BG-11. The maximum cyanobacteria concentrations achieved were 1.10 and 0.76 kg dry cell/m^3 for BG-11 and BG-11_0 media, respectively. The maximum concentration achieved with Allen–Arnon medium was 1.2 kg dry cell/m^3.
2. The time averaged light to biomass energy conversion efficiencies during the growth phase were 7.48%, 5.60%, and 5.75% for BG-11, BG-11_0, and Allen–Arnon medium, respectively.
3. No delay in the onset of H_2 production was observed with Allen–Arnon medium as opposed to a 12 h delay for the other media.

4. Light to hydrogen energy conversion efficiency for Allen–Arnon medium was superior by a factor of 5.5 to both BG-11 and BG-11$_0$ and reached a maximum value of 1.32% and a time averaged value of 0.96% over the duration of the hydrogen production stage of 8 days.

5. The larger specific H_2 production rates for Allen–Arnon medium compared with BG-11 and BG-11$_0$ can be attributed to higher heterocyst frequency observed in Allen–Arnon medium. Higher heterocyst differentiation could partly be attributed to higher concentrations of (i) molybdenum, (ii) magnesium, (iii) calcium, and/or (iv) potassium. Finally, the presence of vanadium in Allen–Arnon medium could have induced production of vanadium based nitrogenase which is reported to evolve more hydrogen than molybdenum based one.

6. The maximum specific hydrogen production rate was 7.73 L/kg/h for the Allen–Arnon medium. The corresponding time averaged specific hydrogen production rates was 5.59 L/kg/h.

7. Based on its excellent transmittance in the PAR, acrylic is suitable construction material for photobioreactors to be used in H_2 production employing cyanobacteria.

Finally, the results presented in this study can aid microbiologists design new media for achieving high cyanobacteria concentrations, for high total H_2 production rates, and possibly higher specific H_2 production rates. It is expected that such a medium used in photobioreactors with uniform light delivery system will help further increase the efficiencies.

Acknowledgements

REFERENCES

[1] Prince RC, Kheshgi HS. The photobiological production of hydrogen: potential efficiency and effectiveness as a renewable fuel. Crit Rev Microbiol 2005;31:19–31.

[2] Pinto FAL, Troshina O, Lindblad P. A brief look at three decades of research on cyanobacterial hydrogen evolution. Int J Hydrogen Energy 2002;27:1209–15.

[3] Department of Energy, Joint Genome Institute. ⟨http://www.jgi.doe.gov⟩, Accessed on: April 19, 2007.

[4] Yoon JH, Sim SJ, Kim MS, Park TH. High cell density culture of Anabaena variabilis using repeated injections of carbon dioxide for the production of hydrogen. Int J Hydrogen Energy 2002;27:1265–70.

[5] Hansel A, Lindblad P. Towards optimization of cyanobacteria as biotechnologically relevant producers of molecular hydrogen, a clean and renewable energy source. Appl Microbiol Biotechnol 1998;50:153–60.

[6] Tsygankov AA, Serebryakova LT, Rao KK, Hall DO. Acetylene reduction and hydrogen photoproduction by wild-type and mutant strains of Anabaena at different CO_2 and O_2 concentrations. FEMS Microbiol Lett 1998;167: 13–7.

[7] Borodin VB, Tsygankov AA, Rao KK, Hall DO. Hydrogen production by Anabaena variabilis PK84 under simulated outdoor conditions. Biotechnol Bioeng 2000;69: 478–85.

[8] Happe T, Schutz K, Bohme H. Transcriptional and mutational analysis of the uptake hydrogenase of the filamentous cyanobacterium Anabaena variabilis ATCC 29413. J Biotechnol 2000;182:1624–31.

[9] Sveshnikov DA, Sveshnikova NV, Rao KK, Hall DO. Hydrogen metabolism of mutant forms of Anabaena variabilis in continuous cultures and under nutritional stress. FEMS Microbiol Lett 1997;147:297–301.

[10] Das D, Veziroğlu TN. Hydrogen production by biological processes: a survey of literature. Int J Hydrogen Energy 2001;26:13–28.

[11] Benemann JR. Hydrogen production by microalgae. J Appl Phsycol 2000;12:291–300.

[12] Madamwar D, Garg N, Shah V. Cyanobacterial hydrogen production. World J Microbiol Biotechnol 2000;16(8–9): 757–67.

[13] Melis A. Green alga hydrogen production: process, challenges and prospects. Int J Hydrogen Energy 2002;27: 1217–28.

[14] Markov SA, Thomas AD, Bazin MJ, Hall DO. Photoproduction of hydrogen by cyanobacteria under partial vacuum in batch culture or in a photobioreactor. Int J Hydrogen Energy 1997;22:521–4.

[15] Tsygankov AA, Borodin VB, Rao KK, Hall DO. H_2 photoproduction by batch culture of Anabaena variabilis ATCC 29413 and its mutant PK84 in a photobioreactor. Biotechnol Bioeng 1999;64:709–15.

[16] Yoon JH, Shin JH, Kim MS, Sim SJ, Park TH. Evaluation of conversion efficiency of light to hydrogen energy by Anabaena variabilis. Int J Hydrogen Energy 2006;31:721–7.

[17] Meeks JC. Experimental protocols. ⟨http://microbiology.ucdavis.edu/meekslab/⟩, Accessed on: June 2, 2006.

[18] Berberoğlu H, Pilon L. Experimental measurement of the radiation characteristics of Anabaena variabilis ATCC 29413-U and Rhodobacter sphaeroides ATCC 49419. Int J Hydrogen Energy 2007;32:4772–85.

[19] Mills A. Mass transfer. Upper Saddle River, NJ: Prentice-Hall; 2001.

[20] Erickson LE, Curless CE, Lee HY. Modeling and simulation of photosynthetic microbial growth. Ann NY Acad Sci 1987:308–24.

[21] Hoffman JD. Numerical methods for engineers and scientists. New York, NY: McGraw-Hill; 1998.

[22] Tsygankov AA, Fedorov AS, Kosourov SN, Rao KK. Hydrogen production by cyanobacteria in an automated outdoor photobioreactor under aerobic conditions. Biotechnol Bioeng 2002;80:715–77.

[23] Minkevich IG, Eroshin VK. Productivity and heat generation of fermentation under oxygen limitation. Folia Microbiologica 1973;18:376–85.

[24] Bolton JR. Solar photoproduction of hydrogen, IEA technical report, IEA/H2/TR-96; 1996.

[25] Allison FE, Hoover SR, Morris HJ. Physiological studies with the nitrogen fixing algae Nostoc muscorum. Bot Gazette 1937;98:433–63.

[26] Bolton JR, Hall DO. The maximum efficiency of photosynthesis. Photochem Photobiol 1991;53:545–8.

[27] Berberoğlu H, Yin J, Pilon L. Simulating light transfer in a bubble sparged photobioreactor for simultaneous hydrogen fuel production and CO_2 mitigation. Int J Hydrogen Energy 2007;32:2273–85.

[28] Kentemich T, Danneberg G, Hundeshagen B, Bothe H. Evidence for the occurrence of the alternative, vanadium-containing nitrogenase in the cyanobacterium *Anabaena variabilis*. FEMS Microbiol Lett 1988;51:19–24.

[29] Kang RJ, Shi DJ, Cong W, Cai ZL, Ouyang F. Regulation of CO_2 on heterocyst differentiation and nitrate uptake in the cyanobacterium *Anabaena* sp. PCC 7120. J Appl Microbiol 2005;98:693–8.

[30] Akkerman I, Jansen M, Rocha J, Wijffels RH. Photo-biological hydrogen production: photochemical efficiency and bioreactor design. Int J Hydrogen Energy 2002;27:1195–208.